Filtration of Flocculated Suspensions Under Declining Pressure

A. D. Martin
Dept. of Chemical Engineering, UMIST, Sackville Street, Manchester, M60 1QD, U.K.

DOI 10.1002/aic.10129
Published online in Wiley InterScience (www.interscience.wiley.com).

The modeling of gravity driven batch filtration is dicussed in which the slurry is considered to comprise a flocculated suspension. The gravity belt thickener and the sludge drying bed are commonly employed devices to which this model may be applied. In both devices, the slurry is applied to a filter medium through which the filtrate passes under the influence of the hydraulic head of the slurry. The solids are retained on the filter and accumulate in up to 3 distinct zones. A fourth zone of clear liquor may also exist above the solids zones. As the filtration process proceeds, the hydraulic head declines because of the discharge of filtrate. A model of this filtration process is developed together with methods for its solution. The model links the filtration rate to the physical properties of the slurry through constitutive relationships for the permeability and compressive yield stress.
 AIChE J, 50: 1418–1430, 2004
Keywords: Gravity filtration, belt thickeners, belt filters, drying beds, flocculated suspension

Objective

The objective of modeling filtration under declining pressure is to establish the relationship between the rate of filtrate flow, the slurry physical properties and the design parameters of the device. This knowledge can be used to improve the design of sludge "drying" beds and more, particularly, gravity belt thickeners.

Introduction

The gravity belt thickener (GBT) is a commonly used device for increasing the solids content of wastewater treatment sludge from approximately 1% to approximately 8%. A film of "thin" sludge is applied to a moving belt of filter cloth. As the belt moves, from the feed end of the device to the discharge end, filtrate passes through the filter cloth, resulting in a reduced slurry film thickness with a higher concentration of solids. The filtrate is collected from the underside of the belt and returned to the wastewater treatment process for further purification. After an initial period of filtration, the partially developed slurry film is "turned over" by sets of fixed ploughs. To facilitate the filtration process, high concentrations of both coagulants and flocculants are added to the thin sludge. These materials, particularly the flocculants are costly and dominate the operating budgets of GBTs. Inappropriate application of the chemical adjuncts can dramatically affect the performance of a particular device. Currently, the adjunct application rates and slurry loading rates for GBTs are established empirically on the full-scale machine. This process must be repeated each time the equipment operators choose to change their adjunct suppliers.

The term "drying bed" is something of a misnomer, since the principal concentration increase occurs as a result of the discharge of "filtrate" through the floor of the bed to the under drains. In operation the drying bed is charged periodically with "thin" sludge, and permitted to stand under quiescent conditions for a period of time. During this stage the solids settle through the liquor under the influence of gravity, while the liquor itself simultaneously permeates through the sand floor of the bed into the drains. Both these processes occur on the belt of a GBT, although the former is less apparent. The design of drying beds is based on empirical considerations and corporate rules of thumb, which completely ignore the rheological properties of the sludge being thickened. Although this design

A. D. Martin's email address is alastair.martin@umist.ac.uk.

approach has been adequate in the past, it is becoming increasingly unreliable because of the addition of adjuncts to enhance the performance of the wastewater treatment plant ahead of the sludge treatment unit.

A one-dimensional (1-D) model will be developed here, which will ignore the effects of shear on the sludge, it will also ignore inertia effects. These assumptions have only limited impact on the applicability of the model to the drying bed, but restrict its application to idealised plug flow between the loading point and the first set of ploughs on the GBT. The development will also assume that the surface tension forces generated between the solid, liquid, and air are always sufficient to support the pendant column of liquid contained in the slurry. Thus, cake "de-saturation" or the first stages of "drying" will be out side the scope of the model.

Sludge arising from wastewater treatment falls into two classes; stable suspensions and flocculated suspensions. It is the latter class of suspension that is of interest here. Stable suspensions are generally produced from the primary sedimentation of raw sewage. However, activated sludge is characteristically flocculated.

In stable suspensions, repulsive forces between the individual particles give rise to an osmotic pressure, which is dependent on the particle concentration or interparticle separation. The addition of coagulant materials to a stable suspension introduces additional van der Waals forces that overcome the existing repulsive forces. The particles then aggregate into clumps or flocs separated by clear liquor. This is a flocculated suspension. Increasing the concentration of the flocculated suspension brings the flocs together until a structure is formed which fills the enclosing vessel. This is the so-called gel point. ϕ_{gel}. As the concentration is increased further, the interaction of the particles in the structure gives rise to a solid-particle pressure, and the solid develops the ability to transmit an applied stress. Under networked conditions the structure is able to support its own weight up to a point. Beyond this point the structure deforms irreversibly, that is, it fails. The point at which failure occurs is known as the compressive yield stress, and is found to be a function of solids concentration, $p_Y(\phi)$. Various functional forms have been used to describe the variation of the yield stress with the concentration of solids. Equation 1 illustrates the form used to describe the wastewater sludge under consideration here (Howells et al., 1990).

$$p_Y(\phi) = \begin{cases} 0, & \phi \le \phi_{gel} \\ k(\phi - \phi_{gel})^m, & \phi > \phi_{gel} \end{cases} \quad (1)$$

Force balance sedimentation filtration theory

There are three types of force present in a suspension that are relevant to filtration and sedimentation.

- Hydrodynamic drag.
- Gravitational and buoyancy.
- Liquid and solid pressure gradients.

In common with previous analyses (Auzerais et al., 1988; Buscall and White, 1987; Bürger and Concha, 1998; Landman et al., 1991), it is assumed that inertial forces are insignificant. Using the three force types to describe the 1-D system shown in Figure 1, two force balances may be drawn up relating to the liquid and solid phases (Eqs. 2, and 3, respectively)

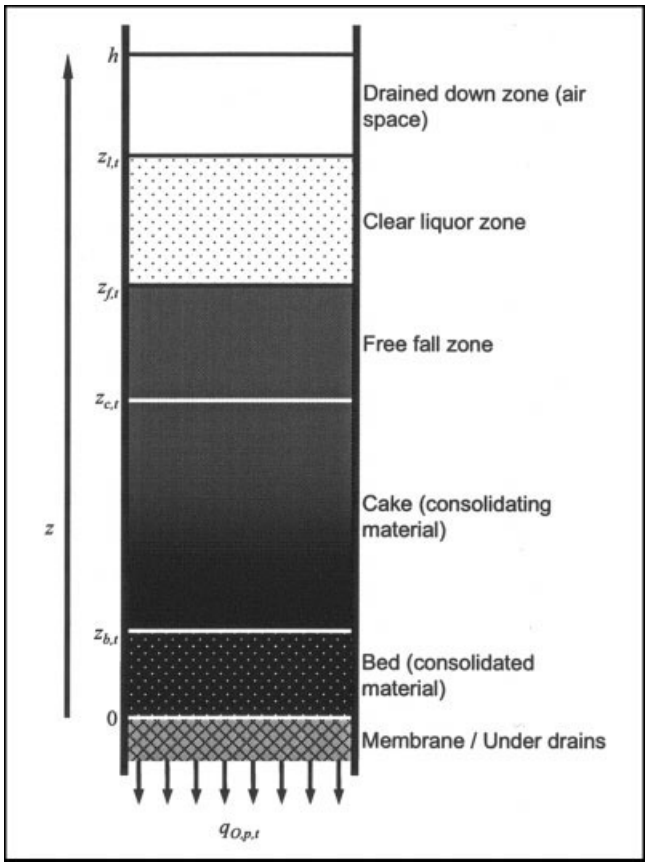

Figure 1. Modeled domain.

$$f_{St}\phi r(\phi)(u - w) - (1 - \phi)\rho_L g - (1 - \phi)\frac{\partial p_L}{\partial z} = 0 \quad (2)$$

$$-f_{St}\phi r(\phi)(u - w) - \phi\rho_S g - \phi\frac{\partial p_L}{\partial z} - \frac{\partial p_S}{\partial z} = 0 \quad (3)$$

where the terms in each equation describe the following forces per unit volume of suspension:

(1) Hydrodynamic drag arising from the relative motion of the solid and liquid phases.
(2) Gravitational force on the individual phases.
(3) Liquid pressure gradient.
(4) Solids pressure gradient, found in Eq. 3 only.

The hydrodynamic drag is characterized by the Stokes-drag coefficient for an isolated sphere, f_{St} ,and a concentration dependent hindered settling factor $r(\phi)$. A power law form of the hindered settling factor as developed by Richardson and Zaki (1954) will be used here (Eq. 4)

$$r(\phi) = (1 - \phi)^j \quad (4)$$

The liquid pressure gradients may be eliminated from the force balance by combining Eqs 2, 3 to yield Eq. 5

$$\frac{f_{St}\phi r(\phi)}{(1 - \phi)}(u - w) + \phi\Delta\rho g + \frac{\partial p_S}{\partial z} = 0 \quad (5)$$

where the system is assumed to be a constant cross section throughout the height of the column of slurry, it is possible to eliminate the liquid velocity in favor of the externally measurable, overall permeate flux, by introducing the overall system mass balance (Eq. 6)

$$0 = u\phi + w(1 - \phi) - q_{O,p} \tag{6}$$

This action leads to Eq. 7

$$\frac{f_{St}\phi r(\phi)}{(1 - \phi)^2}(u - q_{O,p}) + \phi\Delta\rho g + \frac{\partial p_S}{\partial z} = 0 \tag{7}$$

The description of the system is completed with the inclusion of the local mass balance or continuity equation

$$\frac{\partial \phi}{\partial t} = -\frac{\partial(q_S)}{\partial z} \tag{8}$$

Filtration Zones

Filtration of a slurry on a gravity belt filter or a "drying" bed, may result in the formation of up to four transient regions within the slurry column: clear liquor, free fall, cake, and consolidated bed. The existence of any particular region is dependent on the relative rates of sedimentation and filtration. In batch sedimentation 3 regions can be identified, the consolidated bed being absent (Howells et al., 1990). The overall pressure at the base of the slurry column is constant with time, whereas the solids pressure rises. In the absence of gravity, as in simple pressure filtration, a maximum of 2 regions are identified, the clear liquor and the consolidated bed being absent (Landman et al., 1991). As with sedimentation the solids pressure at the membrane rises with time. Filtration at high constant pressure in the presence of gravity was considered by Landman and Russel (Landman and Russel, 1993). Their model identified 3 filtration zones, but, as a consequence of the assumption that the applied pressure was very much greater than the pressure developed due to the weight of the column of sludge, failed to identify the fourth filtration zone, the consolidated bed. In effect, they assumed that, as the gravitational component diminished, it was replaced by an equivalent additional applied pressure. Filtration on a GBT or a drying bed occurs as a result of the weight of the slurry column alone, hence, the assumption made by Landman and Russel must be removed. This leads directly to the possibility of a fourth filtration zone, the consolidated bed. The following subsections will deal with each region in ascending order.

Consolidated bed

The consolidated bed is defined by the region adjacent to the membrane in which the solids pressure is less than the yield stress of the solid network. This zone is characterized by time-independent but spatially variable solids concentration. The condition for the existence of the consolidated bed is stated in Eq. 9

$$p_{S,0,t} < p_Y(\phi_{0,t}) \tag{9}$$

The consolidated bed is bounded by the filtration membrane at $z=0$, and the interface with the consolidating cake above at $z=z_b$. Within the consolidated bed, the yield stress of the solid mass $p_Y(\phi)$ exceeds the solids pressure p_s, hence, there is no relative motion of the solid particles. The zone may be "absent" or have either a "fleeting" or "permanent" existence. A "fleeting" consolidated bed comes into existence early during the filtration, and is, subsequently eroded away before the terminal condition of the filtration is achieved. A "permanent" consolidated bed remains beyond the establishment of the terminal condition. The terminal condition of the system is simply the solids concentration profile achieved at the time filtrate ceases to flow from the base of the slurry column. This concentration profile depends on the entire history of the filtration, and may, in the presence of a "permanent" consolidated bed, differ considerably from the so-called equilibrium condition. As a general rule the terminal condition bed is more compact than its equilibrium equivalent.

The height and composition of the slurry column determine the total pressure at the lower boundary of the consolidated bed. The pressure is evaluated from the integral of the column density between $z=0$ and $z=z_l$

$$\int_0^{z_{l,t}} ((1-\phi_{z,t})\rho_L + \phi_{z,t}\rho_S)\, g dz = p_{L,0,t} + p_{S,0,t} \tag{10}$$

The properties of the filtration membrane of the GBT, or the detailed structure of the drying bed under drains define the liquid pressure at the same location. These structures will be characterized by a simple flow resistance, proportionality constant b_m

$$p_{L,0,t} = -q_{O,p,t} b_m \tag{11}$$

Combining Eqs. 10 and 11 yields a relationship between the solids pressure at the filtration membrane, and the filtrate flow rate (Eq. 12)

$$p_{S,0,t} = \int_0^{z_{l,t}} ((1-\phi_{z,t})\rho_L + \phi_{z,t}\rho_S)\, g dz + q_{O,p,t} b_m \tag{12}$$

For a generalized membrane, the solids flux through the membrane is related to the total filtrate flux, $q_{o,p,t}$, via the filtrate or permeate composition (Eq. 13)

$$u_{0,t}\phi_{0,t} = q_{O,p,t}\phi_p \tag{13}$$

The permeate solids concentration will, however, be assumed to be zero; to do otherwise introduces complexities which are beyond the scope of this article. This assumption, apart from making the problem tractable, is also reasonable from a practical point of view. The solids concentration in GBT permeate is typically less than 200 mg/L, whereas the feed slurry solids composition is nearly 2 orders of magnitude greater at approximately 1%. This assumption constitutes the perfect membrane boundary condition, and two corollaries follow from it:

(1) The solids velocity throughout the consolidated bed is zero.

(2) The entire mass of solids are retained on the filter throughout the process.

Based on these corollaries and the further assumption of homogeneous starting conditions, the integral in Eq. 12 can be very simply evaluated (Eq. 14)

$$\int_0^{z_{l,t}} ((1-\phi_{z,t})\rho_L+\phi_{z,t}\rho_S)\, g dz = z_{l,t}\rho_L g + z_{h,0}\Delta\rho\phi_{z,0} g \qquad (14)$$

Hence, the solids pressure on the lower boundary of the consolidated bed is given by the simple arithmetic expression, Eq. 15

$$p_{S,0,t} = z_{l,t}\rho_L g + z_{h,0}\Delta\rho\phi_{z,0} g + q_{O,p,t} b_m \qquad (15)$$

The upper boundary of the bed is defined by the position at which the cake yield stress is equal to the solids pressure. This condition is given by Eq. 16

$$p_{S,b,t} = p_Y(\phi_{b,t}) \qquad (16)$$

The value of $p_{S,b,t}$ is obtained by substituting the perfect membrane condition into the combined force balance, Eq. 7 to yield Eq. 17

$$\frac{\partial p_s}{\partial z} = \frac{f_{St}\phi\, r(\phi)}{(1-\phi)^2} q_{O,p} - \phi\Delta\rho g \qquad (17)$$

Equation 17 is now integrated over the height of the consolidated bed.

Consolidating cake

The consolidating cake is characterized by time and spatially variable solids concentration. It is defined by the region throughout which the solids pressure is assumed to be equal to the cake yield stress (Buscall and White, 1987)

$$p_S = p_Y(\phi_{z,t}), \quad z_{b,t} < z < z_{c,t} \qquad (18)$$

This assumption was examined by Landman et al. (Landman et al., 1988), and found to be valid to a very high degree of approximation. For the consolidating zone to exist, the following condition must be satisfied

$$z_{h,0}(\rho_L + \Delta\rho\phi_{z,0})\, g > p_Y(\phi_{0,0}) \qquad (19)$$

The lower boundary of the consolidating cake is defined by the upper boundary of the consolidated bed. The upper boundary of the consolidating cake is defined by the point at which the solids pressure falls to the compressive yield stress of the initial slurry. This condition is given by Eq. 19

$$p_{S,c,t} = p_Y(\phi_{0,0}) \qquad (20)$$

Substituting the consolidating cake assumption, Eq. 18, into Eq. 20, it can be deduced that the following condition also holds at the upper boundary of the cake

$$\phi_{c,t} = \phi_{0,0} \qquad (21)$$

Values for $\phi_{c,t}$ are obtained by substituting the consolidating cake assumption into the combined force balance, Eq. 7

$$\frac{f_{St}\phi r(\phi)}{(1-\phi)^2}(u - q_{O,p}) + \phi\Delta\rho g + p'_Y(\phi)\frac{\partial\phi}{\partial z} = 0 \qquad (22)$$

Equation 22 is now integrated simultaneously with Eq. 8 over the consolidating cake region to yield $\phi_{S,c,t}$, $q_{S,c,t}$ and $z_{c,t}$. After introducing zero values for the solids velocity u, and the filtrate flux $q_{O,p}$, Eq. 22 may be integrated between $z=0$ and $z=z_{c,\infty}$ to yield the equilibrium condition solids concentration profile. This is not necessarily the terminal condition solids concentration profile.

Free fall zone

The free fall zone can exist in two states. In both instances the concentration of solids and the solids flux is uniform throughout the zone. The first state is that of a flocculated suspension, and the second state is that of a gelled network. The free fall zone initially occupies the entire height of the slurry column, but diminishes in size throughout the filtration process, and may under certain circumstances disappear before consolidation is complete. It is defined by the region in which the solids pressure is either zero for a flocculated suspension, or less than the yield stress of the network for gelled feed slurry. The region is characterized by time-independent spatially invariant concentration. For a free fall zone to exist the following condition must be satisfied

$$-p_{L,f,t} < p_Y(\phi_{f,t}) \qquad (23)$$

where $p_{L,f,t}$ is obtained from consideration of the overall pressure in the sludge column, and is given by Eq. 24

$$p_{L,f,t} = (z_{l,t} - z_{f,t})\rho_L g - p_{S,f,t} \qquad (24)$$

The form of Eq. 24 is sufficiently general to accommodate the flocculated and gelled states of the free fall zone, as well as the period after the elimination of the clear liquor zone during which the magnitude of $p_{L,f,t}$ rises to the yield stress of the gelled network. The lower boundary of the free fall zone is defined by the upper boundary of the consolidating cake. The upper boundary of the free fall zone is defined by the mass balance, which for the perfect membrane case is given by the following integral

$$\int_0^{z_{f,t}} \phi_{z,t} dz = z_{h,0}\phi_{z,0} \qquad (25)$$

The integral may be split into two parts that may be integrated separately (Eq. 26)

$$\int_0^{z_{c,t}} \phi_{z,t}dz + \int_{z_{c,t}}^{z_{f,t}} \phi_{z,t}dz = z_{h,0}\phi_{z,0} \tag{26}$$

The second integral, relating to the free fall zone is trivially evaluated to yield the expression in Eq. 27

$$\int_0^{z_{c,t}} \phi_{z,t}dz + (z_{f,t} - z_{c,t})\phi_{0,0} = z_{h,0}\phi_{z,0} \tag{27}$$

The solids velocity and, hence, the solids flux in the free fall zone can be defined in terms of the motion of the upper boundary (Eq. 28)

$$\phi_{f,t}\frac{dz_{f,t}}{dt} = \phi_{f,t}u_{f,t} = q_{S,f,t} \tag{28}$$

Two further alternative methods of calculating the solids flux in the free fall zone may be derived for the flocculated suspension and the gelled network. The compressive yield stress of a flocculated suspension is zero and, therefore, solids pressure is also uniformly zero. Substituting this into the combined force balance, Eq. 7 yields the following expression for the solids flux in the free fall zone

$$\phi_{0,0}q_{O,p} - \frac{(1-\phi_{0,0})^2}{f_{St}r(\phi_{0,0})}\phi_{0,0}\Delta\rho g = \phi_{0,0}u_{f,t} = q_{S,f,t} \tag{29}$$

For the gelled network integrating Eq. 7 with constant $\phi = \phi_{0,0}$ followed by rearrangement yields Eq 30 for the free falling solids flux

$$\phi_{0,0}q_{O,p} - \frac{(1-\phi_{0,0})^2}{f_{St}r(\phi_{0,0})}\left\{\phi_{0,0}\Delta\rho g - \frac{p_Y(\phi_{0,0})}{(z_{f,t}-z_{c,t})}\right\} = \phi_{0,0}u_{f,t} = q_{S,f,t} \tag{30}$$

The result in Eq. 30 is valid for both flocculated suspension and gelled network feeds, and only fails when $z_{c,t} = z_{f,t}$ this also corresponds to the condition set out in Eq. 20, above.

Clear liquor Zone

The clear liquor zone is defined as the region of zero solids concentration lying above the free fall zone. It is characterized by time variant, but spatially uniform liquid flux. For the clear liquor zone to develop the column of slurry must be able to consolidate under its own weight, and in the absence of the influence of the liquid weight or the hydraulic gradient, arising from liquid drainage. This initial condition is described by Eq. 31, which states that the yield stress of the initial solids network is less than the solids pressure developed in the network by its self weight

$$p_Y(\phi_{0,0}) < \phi_{0,0}\Delta\rho g(z_{f,0} - z_{c,0}) \tag{31}$$

The upper boundary of the clear liquor zone is the free surface of the liquid. The motion of this boundary is derived by reference to the overall mass balance

$$\frac{dz_{l,t}}{dt} = q_{O,p,t} \tag{32}$$

Summary of the model

Equations 8, 15, 16, 17, 21, 22, 27, 28, 29,30, and 32 constitute the complete description of the declining pressure filtration model. The moments when the conditions 23 and 31 cease to be true define critical events in the filtration process. The former defines the moment at which cake development completes t_f, whereas the latter defines the moment at which the clear liquor finishes draining through the developing free fall or cake zones t_l. For times greater than t_f, the upper boundaries of the free fall and consolidating zones combine. Similarly, for times greater than t_l, the upper boundaries of the clear liquor and free fall zones combine, and for $t \geq \max(t_f, t_l)$, all three boundaries are combined, and cake consolidation or compression commences. t_l also marks the onset of "capillary" assisted thickening during which part of the weight of the liquid column is transferred to the solids at the three-phase interface $z_{l,t}$.

Normalization of the filtration equations

It is convenient to draw sets of parameters together into dimensionless groups. To do this a development of Howells (Howells et al., 1990) approach is used

$$\Phi = \frac{\phi}{\phi_n} \quad Z = \frac{z}{h} \quad P_S = \frac{p_S}{p_Y(\phi_n)} \quad P_Y(\Phi) = \frac{p_Y(\phi)}{p_Y(\phi_n)}$$

$$B(\Phi) = \frac{(1-\phi)^2 r(\phi_n)}{(1-\phi_n)^2 r(\phi)} \quad B_m = \frac{f_{St}h\phi_n r(\phi_n)}{(1-\phi_n)^2 b_m}$$

$$U = \frac{f_{St}h\phi_n r(\phi_n)u}{p_Y(\phi_n)(1-\phi_n)^2} \quad Q = \frac{f_{St}hr(\phi_n)q}{p_Y(\phi_n)(1-\phi_n)^2}$$

$$T = \frac{p_Y(\phi_n)(1-\phi)^2 t}{f_{St}\phi_n r(\phi_n)h^2} \quad \varepsilon = \frac{p_Y(\phi_n)}{\phi_n h\Delta\rho g} \quad \eta = \frac{p_Y(\phi_n)}{h\rho_L g}$$

Equation 8:
$$\frac{\partial\Phi}{\partial T} = -\frac{\partial Q_S}{\partial Z} \tag{33}$$

Equation 15:
$$P_{S,0,T} = \frac{Z_{l,T}}{\eta} + \frac{\Phi_{0,0}}{\varepsilon} + \frac{Q_{O,p,T}}{B_m} \tag{34}$$

Equation 16:
$$P_{S,b,T} = P_Y(\Phi_{b,T}) \tag{35}$$

Equation 17:
$$\frac{\partial P_S}{\partial Z} = \frac{\Phi Q_{O,p,T}}{B(\Phi)} - \frac{\Phi}{\varepsilon} \tag{36}$$

Equation 21:
$$\Phi_{c,T} = \Phi_{0,0} \tag{37}$$

Equation 22:
$$\frac{\partial\Phi}{\partial Z} = -\frac{(Q_S - \Phi Q_{O,p,T})}{B(\Phi)P'_Y(\Phi)} - \frac{\Phi}{\varepsilon P'_Y(\Phi)} \tag{38}$$

Equation 27: $$\int_0^{Z_{c,t}} \Phi_{Z,T} dZ + \Phi_{0,0}(Z_{f,T} - Z_{c,T}) = \Phi_{0,0} \quad (39)$$

Equation 28: $$\Phi_{f,T} \frac{dZ_{f,T}}{dT} = Q_{S,f,T} \quad (40)$$

Equation 29: $$\Phi_{0,0} Q_{O,p,T} - B(\Phi_{0,0}) \frac{\Phi_{0,0}}{\varepsilon} = Q_{S,f,T} \quad (41)$$

Equation 30: $$\Phi_{0,0} Q_{O,p,T} - B(\Phi_{0,0}) \left\{ \frac{\Phi_{0,0}}{\varepsilon} + \frac{P_Y(\Phi_{0,0})}{(Z_{c,T} - Z_{f,T})} \right\} = Q_{S,f,T} \quad (42)$$

Equation 32: $$\frac{dZ_{l,T}}{dt} = Q_{O,p,T} \quad (43)$$

Conditions

Equation 23: $$-P_{L,f,T} < P_Y(\Phi_{f,T}) \quad (44)$$

Equation 31: $$P_y(\Phi_{0,0}) < \frac{\Phi}{\varepsilon}(Z_{f,0} - Z_{c,0}) \quad (45)$$

Numerical solution algorithm

The numerical solution of the model represented by Eqs 33 to 43, and conditions 44 and 45, requires integration in the spatial dimension and in the time dimension. These integrations must be carried out concurrently. The first step in the development of the numerical algorithm is to discretise the time derivatives. A first-order backward difference method, based on a discrete time interval,ΔT is chosen

$$\left.\frac{dZ_l}{dT}\right|_T = \frac{Z_{l,T} - Z_{l,T-\Delta T}}{\Delta T} \quad (46)$$

$$\left.\frac{dZ_f}{dT}\right|_T = \frac{Z_{f,T} - Z_{f,T-\Delta T}}{\Delta T} \quad (47)$$

$$\left.\frac{d\Phi}{dT}\right|_T = \frac{\Phi_T - \Phi_{T-\Delta T}}{\Delta T} \quad (48)$$

Substituting for the time derivative in Eq. 33 yields the discrete approximation for the spatial derivative of the solids flux

$$\left.\frac{dQ_S}{dZ}\right|_T = \frac{\Phi_T - \Phi_{T-\Delta T}}{\Delta T} \quad (49)$$

The solution of the set of equations is now achieved by propagating the known state at $T-\Delta T$ to the new state at T. The solution objective at each state is the flux of permeate $Q_{O,p,T}$. The method chosen to propagate the solution from one state to the next is a first-order Euler algorithm. Solution in the spatial dimension at each time step is achieved with the iterative scheme outlined in Figure 2. The "Solver 1" case illustrated is relevant to the initial condition $p_Y(\phi_{0,0}) < \phi_{0,0}/\varepsilon$, that is, solids settling through the liquid. Three further solver cases are required, which differ in detail from "Solver 1". Table 1 sets out the key differences.

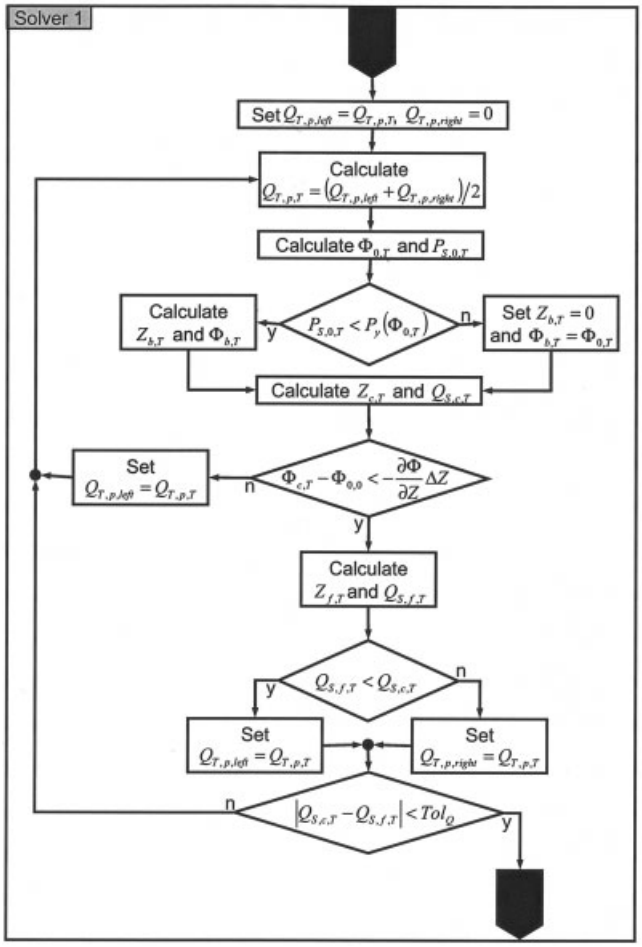

Figure 2. Flow of calculation procedure within a sample solver

Integration in the spatial domain was achieved with a 4th-5th order Runge-Kutta method was chosen because of its ability to rigorously estimate the magnitude of the 4th order round off error, and implement automatic step-size adjustment. The implementation was adapted from the Cash-Karp Runge-Kutta methods "rkqs" and "rkck" (Press et al., 1996). While a simple 4th-order method would have been adequate in terms of precision, the computational efficiency and additional stability conferred on the solution by the mixed order method significantly out-weighed the penalty of additional complexity. Due to the lack of *a priori* knowledge of the functional form of the solution, and the relative ease with which upper and lower bracketing values can be established, a simple interval halving iterative method is chosen for evaluating $Q_{O,p,T}$. The solution procedure shown in Figure 2 is generally similar to that of Howells et al. (Howells et al., 1990). As the solution evolves, the top boundary at $Z_{l,T}$ may converge with the boundary at the top of the solids free fall zone $Z_{f,T}$ and ultimately with the top of the consolidating zone $Z_{c,T}$. This compounding of the upper

Table 1. Summary of Functional Difference Between Solvers

	Solver 1	Solver 2	Solver 3	Solver 4
Domain of applicability	Clear liquor and free-fall zones present $T < \min(T_f, T_l)$	Clear liquor zone present, free-fall zone absent $T_f < T < T_l$, $\Phi_{0,0} < \Phi_{gel}$	Clear liquor zone absent, free-fall zone present $T_l < T < T_f$, $\Phi_{0,0} > \Phi_{gel}$	Clear liquor and free-fall zones absent $T > \max(T_f, T_l)$
Determination criteria for $Z_{c,T}$	$\frac{d\Phi}{dZ} \le 0, \Phi_{c,T} - \max(\Phi_{0,0}, \Phi_{gel}) < -\frac{d\Phi}{dZ}\Delta Z$	$\frac{d\Phi}{dZ} \le 0, M_{c,T} = \Phi_{0,0} Z_{f,0}$	$\frac{d\Phi}{dZ} \le 0,$ $\Phi_{c,T} - \Phi_{0,0} < -\frac{d\Phi}{dZ}\Delta Z$	$\frac{d\Phi}{dZ} \le 0, M_{c,T} = \Phi_{0,0} Z_{f,0}$
Calculation of $Q_{S,f,T}$	$\Phi_{0,0} Q_{O,p,T} - B(\Phi_{0,0})\left(\frac{\Phi_{0,0}}{\varepsilon} - \frac{P_Y(\Phi_{0,0})}{(Z_{f,T} - Z_{c,T})}\right)$	$\Phi_{gel}\frac{Z_{f,T} - Z_{f,T-\Delta T}}{\Delta T}$	$\Phi_{0,0} Q_{O,p,T}$	$\Phi_{c,T-\Delta T} Q_{O,p,T}$

boundary requires subtly different treatment in the numerical solution (Table 1). The transitions equate to changes in the filtration behavior. Figure 3 illustrates the solution process in the time domain showing the inter-relationship of the four solvers, and the application of the decision criteria to the resolution of critical times T_f and T_l. In the following sections selected steps will be examined in additional detail.

Solution over the consolidated bed

The consolidated bed may begin to develop when the filtration is initiated. If the conditions for the existence of a consolidated bed exist when the filtration is initiated then the process will cease immediately. The objectives of the solution in this zone are to establish the height of the consolidated bed $Z_{b,T}$, the concentration of solids at the top of the bed $\Phi_{b,T}$ and the mass of solids contained in the bed $M_{s,b,T}$. The solids composition within the consolidated bed is invariant with time; hence, the integration of Eq. 36 proceeds using the previously calculated solids concentration profile. The 4th-5th order Runge-Kutta method is employed for this process. Where concentration values are required at points intermediate to the imposed grid, a simple two-point linear interpolation method is used. The integration continues until $P_{S,Z,T}$ exceeds $P_Y(\Phi_{Z,T})$. This establishes the grid points that bracket the estimate of $Z_{b,T}$. An interval halving method is then systematically applied to the "brackets" until satisfactory approximations to the position of the boundary and the condition in Eq. 35, are achieved. A consistent selection of a "valid" result, that is, $P_{S,Z,T} \le P_Y(\Phi_{Z,T})$, has been found to produce a more stable solution to the overall problem.

The mass of solids contained in the bed, $M_{S,b,T}$, is calculated by integrating the solids concentration profile between the limits $Z=0$ and $Z=Z_{b,T}$. The result has no direct baring on this part of the solution, but becomes vital in the later stages of the spatial integration.

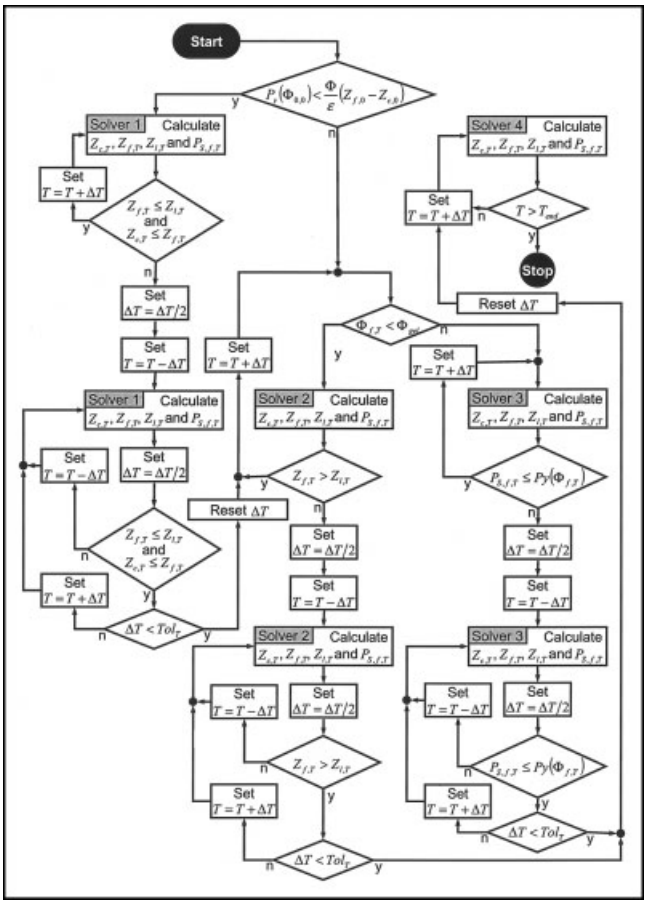

Figure 3. Flow of calculation between solvers and resolution of critical times

Solution over the consolidating cake

The solution in the consolidating cake region requires the simultaneous integration of Eqs. 33 and 38. As with the consolidated bed, a 4th -5th order Runge-Kutta method is used. The objectives of this stage are to establish the height of the top of the cake above the membrane $Z_{c,T}$, the concentration of solids at the top of the cake $\Phi_{c,T}$, and the mass of solids contained in the cake and bed zones combined $M_{S,c,T}$. In the early stages of the solution, $T<T_f$, the value of $\Phi_{c,T}$ is known in advance to be equal to the maximum of $\Phi_{0,0}$ and Φ_{gel}. Under these circumstances, integration proceeds until $\Phi_{z,T}$ is less than either $\Phi_{0,0}$ or Φ_{gel}. Unfortunately, the behavior of the solution is such that this condition cannot be established for all estimates of $Q_{O,p,T}$, hence, it is impossible to reliably establish a value of $Z_{c,T}$. An additional property of the solution, indicated by Eq 50, can be drawn on to establish a value of $Z_{c,T}$ for all estimates of $Q_{O,p,T}$

$$\frac{\partial \Phi}{\partial Z} = -\frac{(Q_S - \Phi Q_{O,p,T})}{B(\Phi)\,P'_Y(\Phi)} - \frac{\Phi}{\varepsilon P'_Y(\Phi)} = 0 \qquad (50)$$

This condition holds for both valid and invalid values of $Z_{c,T}$, hence, an additional test is required to validate the value of $Z_{c,T}$. The behavior of the solution around this turning point is complex. When the free fall zone is large strictly as $(Z_{f,T}-Z_{c,T}) \rightarrow \infty$ and its sedimentation velocity approaches the limiting maximum value, the turning point is poorly located. The spatial derivative of Φ is almost zero over a wide range of values of Z. This condition is typical of the early filtration period of a feed slightly above the gel point. In the later stages of filtration the turning point becomes increasingly tight, and, for values of $\Phi_{0,0} \leq \Phi_{gel}$, it is cusped by virtue of the fact that for the ungelled solid $P'_Y(\Phi) = 0$. These characteristics are such that simply testing for $\Phi_{c,T} > \Phi_{0,0}$ as the integration proceeds is not sufficient to reliably establish the validity of the estimate of $Z_{c,T}$. Instead, it is necessary to apply a more discriminating test, based on the Z derivative of Φ at the last estimate of $Z_{c,T}$

$$\Phi_{c,t} - \Phi_{0,0} > -\left.\frac{\partial \Phi}{\partial Z}\right|_{Z=Z_{c,t}} \Delta Z \tag{51}$$

This test is equivalent to Howells' "test 1" (Howells et al., 1990]), although it is able to discriminate between valid and invalid estimates as Φ approaches Φ_g much more closely than in Howells' method. Howells et al. apply a second test of validity to calculated values of $Z_{c,T}$. Their second test, $Z_{c,T} > Z_{c,T-\Delta T}$, is not valid when $\Phi_{0,0}$ approaches Φ_{gel}, and leads to instabilities in the solution algorithm. Once the grid points bracketing the desired solution have been identified, regardless of the specifics of the boundary condition, simple interval halving is employed to refine the estimates of $Z_{c,T}$, $Q_{S,c,T}$, and in the later stages, $\Phi_{c,T}$. With valid estimates of $Z_{c,T}$ and $Q_{S,c,T,}$ it is possible to obtain the solution over the free fall zone, which is discussed in the next section.

Solution over the free fall zone

In the latter stages of filtration $T > T_f$ the free fall zone may cease to exist. Hence, there are two circumstances to be considered when estimating the value of $Z_{f,T}$.

$T < T_f$

When the free fall zone is present, the position of the upper boundary is established by simple application of the mass balance (Eq. 39). Equation 39 requires the evaluation of the integral of the solids concentration profile in the consolidated bed and consolidating zones $M_{S,c,T}$. This can be done independently, but is efficiently and advantageously executed simultaneously with Eqs. 33 and 38.

$T \geq T_f$

Under these circumstances, the free fall zone has ceased to exist, that is, $Z_{f,T} - Z_{c,T} = 0$. It can be seen that the mass balance definition of $Z_{f,T}$, Eq. 39, remains valid. However, it becomes necessary to evaluate the integral in Eq. 39 simultaneously with Eqs. 33 and 38. An additional check is applied to the solution in the consolidating zone; integration is now halted when $M_{S,Z,T}$ exceeds $M_{S,1,0}$.

Once the value of $Z_{f,T}$ has been estimated, the discrete form of Eq. 40 below, is used to calculate the solids flux at the clear liquor interface

$$\Phi_{f,T} \frac{Z_{f,T} - Z_{f,T-\Delta T}}{\Delta T} = Q_{S,f,T} \tag{52}$$

Revision of the Estimate of $Q_{O,p,T}$

Noting that the solids flux is uniform in the free fall zone, and that continuity must be satisfied at the lower boundary, the basis for revision of $Q_{O,p,T}$ is readily established

$$Q_{S,f,T} < Q_{S,c,T} \quad \text{then} \quad Q_{O,p,lower} = Q_{O,p,T} \tag{53}$$

$$Q_{S,f,T} \geq Q_{S,c,T} \quad \text{then} \quad Q_{O,p,upper} = Q_{O,p,T} \tag{54}$$

Also, from these conditions, a basis for convergence can be established

$$|Q_{S,f,T} - Q_{S,c,T}| < Tol(1 - Q_{S,c,T}) \tag{55}$$

The condition set out in Eq. 55 is rather arbitrary, and, as the magnitude of $Q_{S,c,T}$ diminishes, the form of the check moves from a relative convergence to an absolute convergence, which may be unsatisfactory in situations where the solids flux is generally low. For these situations, an alternative form of check may prove suitable

$$Q_{S,c,T} + \frac{\Omega}{Tol} |Q_{S,f,T} - Q_{S,c,T}| = Q_{S,c,T} \tag{56}$$

where Ω is a machine dependent constant equal to approximately 10^{-8} for single precision and 10^{-16} for double precision numbers. The equality is not strict in the mathematical sense, but becomes true in the computational sense when the magnitude of the second term becomes insignificant relative to the first. This form of the convergence check continues to be a relative check regardless of the magnitude of $Q_{S,c,T}$.

Solution over the clear liquor zone

The new value of $Z_{l,T}$ is calculated simply with a rearrangement of the discrete form of Eq.43 to propagate the value at state $T - \Delta T$ to the state at T (Eq. 57)

$$Z_{l,T} = Z_{l,T-\Delta T} + \Delta T Q_{O,p,T} \tag{57}$$

Resolution of critical times

Two critical times have been identified corresponding to the elimination of the clear liquor and free fall zones. The order in which these zones are eliminated can be deduced in advance. It is found that $T_f < T_l$ when $\Phi_{0,0} < \Phi_{gel}$ and vice versa. This gives rise to two alternative conditions of the system in the interval $T_f T_l$. These correspond to $T_f < T < T_l$ and $T_l < T < T_f$. To cover all the the possible conditions of the system, a total of 4 subtly different solvers are required. Table 1 highlights the functional differences, whereas Figure 3 illustrates the flow of the calculation from initiation to conclusion.

Table 2. Parametric Values for Illustrative Case Definitions

	Case 1	Case 2
$\Phi_{0,0}$	0.20	0.35
$P_y(\Phi)$	$m = 2$	
	$\Phi_{gel} = 0.25$	
$B(\Phi)$	$j = 12$	
B_m	118	
ε	2.55	
η	19.62	

Elimination of the clear liquor zone

The condition expressed in Eq. 45 may be converted to a simple test of the relative values of $Z_{l,T}$ and $Z_{f,T}$. An interval halving method can be applied to the time coordinate, and the values of $Z_{l,T}$ and $Z_{f,T}$ converged to a suitable tolerance with the additional proviso that $Z_{l,T} > Z_{f,T}$.

Elimination of the free fall zone

It is known that the pressure at the upper boundary of the consolidating cake is equal to the yield stress of the solid. Hence, by integrating Eq. 38 over the constant composition free fall zone yields Eq. 58 for the solids pressure at its upper boundary

$$P_{S,f,T} = P_Y(\Phi_{0,0}) - \left\{\frac{(Q_{S,c,T} - \Phi_{0,0}Q_{O,p,T})}{B(\Phi_{0,0})} + \frac{\Phi_{0,0}}{\varepsilon}\right\}(Z_{f,T} - Z_{c,T}) \tag{58}$$

Although it may appear to be adequate to simplify the test to checking the relative values of $Z_{f,T}$ and $Z_{c,T}$, this proves to be inadequate as $\Phi_{0,0} \rightarrow \Phi_{gel}$. Under these circumstances, the term in parentheses is poorly determined, but the term in brackets tends to zero, hence, making this test robust compared with the simplified version.

Setting the first bracketing values of $Q_{O,p,T}$ at each time step

To initiate the interval halving algorithm, it is necessary to establish an upper and lower bracket at each time step. The smaller the bracketing interval, the more rapid the overall solution algorithm is likely to be. This has to be considered in the context of the available knowledge of the shape of the expected solution. Through arguments of irreversibility it is deduced that the magnitude of $Q_{O,p,T}$ diminishes throughout the filtration process. However, because of the merging of the various interfaces, it is not possible to deduce anything useful about the time derivative of $Q_{O,p,T}$ which is also consistent throughout the time period. Hence, a very simple although occasionally inefficient bracketing method is employed (Eqs 59 and 60)

$$Q_{O,p,upper} = 0 \tag{59}$$

$$Q_{O,p,lower} = Q_{O,p,T-\Delta T} \tag{60}$$

To initiate the time integration, it is necessary to generate the first pair of brackets. The upper bracket as indicated by Eq. 59 is very conservative, but may be inefficient. The lower bracket is a little more difficult to establish, but can be quantified, based on the boundary condition at the membrane (Eq. 34). Noting that at the initial conditions $P_{S,0,0} = P_Y(\Phi_{0,0})$, Eq. 61, and *that* $Z_{l,0}=1$, Eq. 34 can be rearranged to yield $Q_{O,p,0}$, Eq. 61

$$Q_{O,p,0} = B_m\left\{P_Y(\Phi_{0,0}) - \frac{1}{\eta} - \frac{\Phi_{0,0}}{\varepsilon}\right\} \tag{61}$$

Results

Two illustrative cases are considered:

Case 1: $\Phi_{0,0} < \Phi_{gel}$
Case 2: $\Phi_{0,0} > \Phi_{gel}$

The basic data is set out in Table 2. A high value is selected for B_m so that the permeability of the membrane exerts no detectable influence over results, that is, the membrane can be regarded as resistance free.

Case 1

Figures 4a to 4d summarize the results obtained, while modeling the filtration of a slurry with an initially uniform solids concentration less than the gel concentration, ($\Phi_{0,0} < \phi_g$). The slurry is flocculated. Figure 4a shows the trajectories of the various interfaces. For this flocculated slurry, the solids settle through the liquid initially, while the liquid simultaneously filters through the consolidating cake and consolidated bed. The time to cake completion T_f is as expected less than the time taken to eliminate the clear liquor zone T_l. Once the cake has been completed, which is indicated by the convergence of the consolidation interface Z_c with the clear liquor interface Z_f, the rate of solid settling diminishes rapidly. This is visible in the $Q_{s,c}$ curve of Figure 4b, which plots the evolution of the solids flux at the consolidation interface. The settling rate diminishes, under the influence of the up thrust from the networked solids in the consolidating cake, until after a short period of time it has fallen to less than the filtration rate. From this time onward, the clear liquor zone decreases in size, finally vanishing when Z_f and Z_c converge with Z_l at T_l (Figure. 4a).

Once the clear liquor zone has vanished, it is possible for the liquid to derive some support by virtue of the surface tension forces developed as the initially flat liquor surface deforms over the top of the gelled solids. This leads to the application of pressure to the top of the consolidating cake, precipitating a rapid rise in the solids concentration (Figure 4c), and a commensurate rise in the consolidating solid flux $Q_{S,c}$ (Figure 4b). During the remainder of the final phase of the filtration, the consolidating solid flux and liquid filtration rate $Q_{o,p}$ decline together (Figure 4b), while the solids concentration at Z_c continues to increase steadily (Figure 4c). The solids concentration in the consolidating bed also becomes increasingly uniform through this period (Figure 4d).

During filtration on high permeability membranes, and as a direct consequence of the declining filtration pressure, a bed of consolidated solids develops. The flow resistance of this bed controls the rate of filtration. In Figure 4a, the upper boundary of this bed can be seen to rise initially until it occupies approximately 10% of the initial height of the slurry column,

and approximately 25% of the height at the time the maximum is reached. As the filtration proceeds the upper boundary of the consolidated bed is eroded. This is because of the decline in the liquid pressure drop through the bed, which translates into the development of a greater compression force at the top of the consolidating zone.

Case 2

Figures 5a to 5d summarize the results obtained, while modeling the filtration of a slurry with an initially uniform solids concentration greater than the gel concentration, ($\Phi_{0,0} > \Phi_g$). The slurry is networked from the outset. Figure 5a shows the trajectories of the various interfaces during the course of the filtration. Although the conditions exist for the development of a clear liquor zone, it is evident that its development is very modest and cannot be resolved on a plot of this type. The clear liquor zone is finally eliminated at $T_l = 0.011$. The only visible evidence of this is derived from the sudden gradient change in the $Z_{c,T}$ curve. For $T > T_l$, the pressure arising from the balancing of the surface tension force gradually rises as the pressure drop due to filtrate flow falls, resulting in the steady erosion of the bottom of the free-fall zone. Ultimately, at T_f, the yield stress of the initial solids network is exceeded throughout the height of the solids column, and consolidation occurs leading to an increase in solids concentration at the upper boundary (Figure 5c). Unlike case 1, the solids flux in the interval T_l, T_f diminishes relatively slowly, and there is no rapid increase as cake consolidation commences (Figure 5b). The rise in the solids flux during the consolidation phase is much less marked than for case 1, this merely reflects the greater yield stress of the slurry. It is also worth noting that the final solids content of the slurry is in fact lower than case 1 (Figure 5c), despite the higher initial solids concentration and identical filtration times. This is also confirmed through the calculation of the mean solids concentration $\bar{\Phi}_{0.0508} = 1.54$ for case 1, where as, $\bar{\Phi}_{0.0508} = 1.34$ for case 2. Figure 5d, illustrating the solids concentration distribution in the cake and bed, indicates that a higher equilibrium solids concentration can be

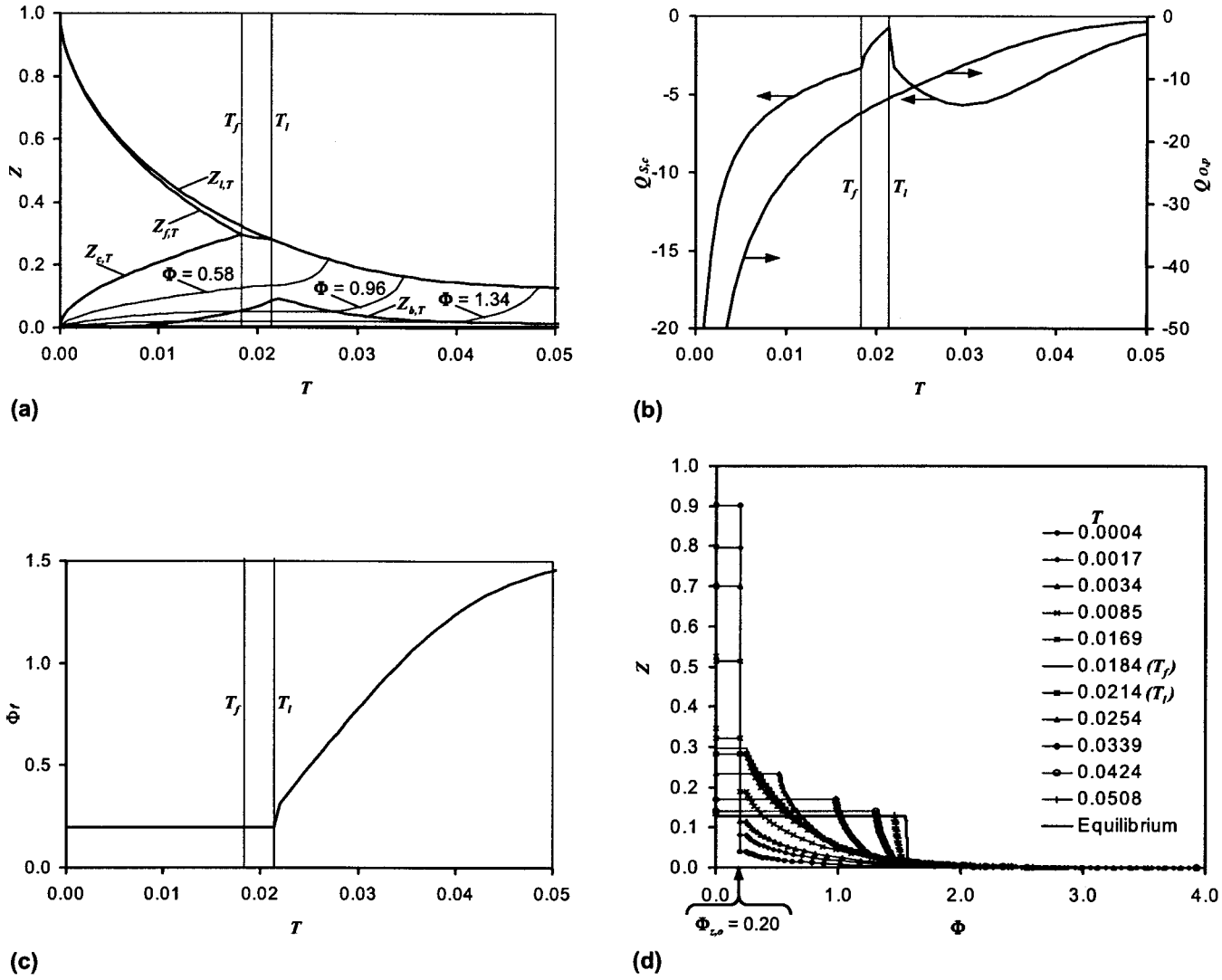

Figure 4. Case 1 results.

(a) Evolution of the filtration zones; (b) evolution of the permeate ($Q_{O,p}$) and consolidating solids ($Q_{S,c}$) fluxes; (c) evolution of the clear liquor interfacial solids concentration (Φ_f), and (d) axial solids concentration profiles.

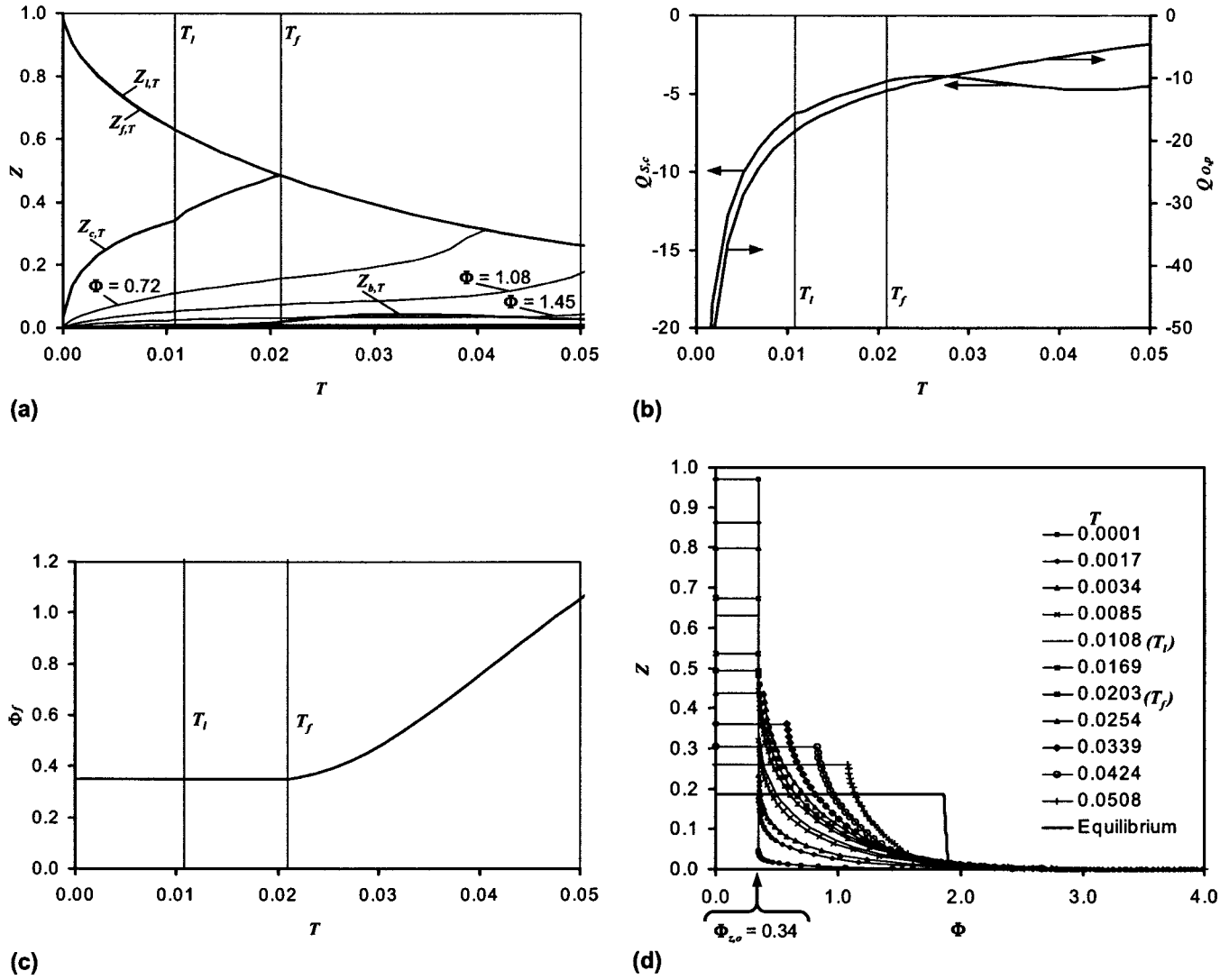

Figure 5. Case 2 results:

(a) Evolution of the filtration zones; (b) evolution of the permeate ($Q_{O,p}$) and consolidating solids ($Q_{S,c}$) fluxes; (c) evolution of the clear liquor interfacial solids concentration (Φ_f), and (d) axial solids concentration profiles.

achieved in case 2 $\bar{\Phi}_e = 1.88$ than case 1 $\bar{\Phi}_e = 1.57$. This is due to the greater height of the solids column at equilibrium and, therefore, a greater load applied to the top surface of the slurry by the "pendant" column of liquid acting through the surface tension forces. Close examination of the solids concentration distributions in Figure 5d for $T<T_l$ reveals the absence of the Φ_{gel}, $\Phi_{0,0}$ step, evident in Figure 4d.

As with case 1, filtration on an almost ideal membrane leads to the development of a consolidated bed ($Z_{b,T}$, shown in Figure 5a). However, there is a much thinner bed development compared with case 1, only reaching 4.6% of the original height, and 7.9% of the column height at the time of the maximum. This arises from the slightly higher concentration of solids at the membrane in case 2, and the much diminished permeability. The exponent in the permeability function is 12. The thinner consolidated bed of case 2 exerts a much stricter control over the filtration rate than the thicker bed in case 1.

Discussion

Limitations

The model described here assumes that the force arising from the liquid surface tension, and the deformation of the liquid surface over the solid network is always sufficient to support the pendant column of liquid. The stress generated by surface tension effects is proportional to the wetted length per unit area at the slurry, and a function of the contact angle between the liquid and solid phases. The wetted length will be a function of the solids morphology, particle size, and solids concentration. Slurries comprising high concentrations of finely divided, hydrophilic solids, can, therefore, be expected to support large pendant columns of liquid. When deep beds or slurries of coarse particles are considered at long filtration times the surface tension assumption may cease to hold, and the liquid may continue to drain through the solid cake leaving a "dry" bed resting on top of the saturated cake.

The solution method, although capable of functioning successfully closer to the gel point than the sedimentation method of Howells et al. (Howells et al., 1990), becomes increasingly unreliable in the calculation of the values of Z_c and T_f as the gel concentration is approached. This loss of precision is a fundamental property of the problem rather than a characteristic of the solution method. Inspection of Eq. 1 reveals that as the gel point is approached $p_Y(\phi)$, and more importantly $p'_Y(\phi)$ tend to zero. Naturally the dimensionless yield stress and yield stress gradient also tend to zero. Turning to Eq. 38, which defines the spatial concentration gradient, it can be seen that the denominators of both terms on the right-hand side go to zero at the gel point, leaving the spatial concentration gradient undefined. Alternative reasoning suggests that the spatial concentration gradient tends to zero for "just gelled" systems although tending to minus infinity for "just not gelled" systems. Computational experimentation indicates that this property of the solution compromises the calculated values of Z_c and T_f in the range $0.98\Phi_{gel} < \Phi_{0,0} < 1.02\Phi_{gel}$. It is possible that precision close to the gel concentration may be preserved by consideration of the spatial solids pressure gradient rather than the equivalent solids concentration gradient. The lack of precision in the calculation of Z_c and T_f near the gel concentration does not propagate significant instabilities into other parts of the solution, hence, the calculation of the filtrate flux $Q_{o,p}$, for example, remains reliable. A further difficulty arises when modeling just gelled systems. Upon the elimination of the clear liquor zone, the slight increase in the pressure on the upper surface of the free fall zone is sufficient to precipitate almost instantaneous consolidation throughout the zone.

Implications

The results presented here serve to illustrate a few key features of the solution rather than values significant to industrial practice.

Qualitative observation of a GBT in operation reveals a number of features. The slurry is applied to the moving belt as a relatively low viscosity liquid, and rapidly spreads to form an even film. The upper surface of the film may develop a smooth glassy appearance that subsequently becomes rough. In the wake of the first set of ploughs, it is possible to observe the breakup of the dense layer, which the ploughs have raised off the membrane. The slurry then flows to a minor extent forming ridges separated by sections of exposed belt. The ridges are broken up and turned over by further sets of ploughs. The model presented here reproduces the features observable between the application of the slurry and the first set of ploughs, and offers additional interpretation of the glassy and rough surfaces. The glassy surface is indicative of the presence of a clear liquor zone, and that the initial sedimentation rate exceeds the filtration rate. The transition between the glassy surface and the rough surface is not usually distinct because of inhomogeneity in the slurry, but indicates the elimination of the clear liquor zone $T_{,l}$. The development of a dense consolidated layer close to the membrane is also predicted. On an operating GBT, this layer is rather difficult to observe directly, however, its presence can be inferred from observation of the ploughing action. The development of a clear liquor zone has been modeled before (Landman et al., 1993). However, their work investigated filtration at high pressures and, therefore, ignored the effect the "self-weight" of the solids had on the filtration. The results presented here consider very low filtration pressures that decline throughout. The mechanism which gave rise to the clear liquor zone in Landman et al.'s work is seen to apply even at very low filtration pressures, and is simply a function of the strength of the slurry. The longevity and maximum size of this zone are functions of the relative rates of filtration and sedimentation.

Comparison of Figures 4a and 5a shows that increasing the initial solids concentration of the slurry, while maintaining the initial height of the column, leads to the achievement of a lower final solids concentration after a fixed period of filtration. This observation, while initially surprising, is consistent with the findings of Landman and White (Landman and White, 1997) for pressure filters. This aspect of behavior has important implications for operators of GBTs and sludge drying beds. For the operation of a GBT, the operator requires a knowledge of the relationship between the rate of slurry application, initial slurry concentration, and the belt speed to achieve a consistent product quality and throughput. This model, although not complete, provides the foundations for the establishment of such relationships, based on slurry properties which can be determined in the laboratory (DeKretser, 2001).

Notation

B = dimensionless permeability
b = dimensioned resistance, $ML^{-2}T^{-1}$
f_{St} = stokes-drag coefficient, $ML^{-3}T^{-1}$
g = acceleration because of gravity ($9.81 m/s^2$), LT^{-2}
h = dimensioned initial slurry column height (normalization basis), L
j = exponent in slurry flow resistivity model
k = proportionality constant in yield stress model, $ML^{-1}T^{-2}$
M = dimensionless mass below subscripted location
m = exponent in yield stress model
P,p = dimensionless, dimensioned pressure or compressive stress, $ML^{-1}T^{-2}$
Q,q = dimensionless, dimensioned flux, LT^{-1}
r = slurry flow resistivity model
T, t = dimensionless, dimensioned time, T
U, u = dimensionless, dimensioned solids velocity, LT^{-1}
w = dimensioned liquid velocity, LT^{-1}
Z, z = dimensionless, dimensioned height, L

Greek letters

Φ,ϕ = dimensionless, dimensioned solids volume fraction
ϵ = dimensionless sedimentation driving force
η = dimensionless filtration driving force
ρ = density, ML^{-3}

Subscripts

b = relating to the interface between the consolidated bed and the consolidating cake zones
c = relating to the interface between the consolidating cake and the free fall zones
f = relating to the interface between the free fall and the clear liquor zones
gel = relating to the gel point
L = liquid phase
l = relating to the interface between the clear liquor and the drained down zone
m = membrane
n = basis for normalization
O = overall

p = permeate
S = solid phase
T = relating to an instant in dimensionless time
t = relating to an instant in dimensioned time
Y = yield
z = arbitrary vertical position

Literature Cited

Auzerais, F. M., R Jackson, and W. B. Russel, "The Resolution of Shocks and the Effects of Compressible Sediments in Transient Settling," *J. Fluid Mech.*, **196**, 437 (1988).

Bürger, R., and F. Concha, "Mathematical Model and Numerical Simulation of the Settling of Flocculated Suspensions," *Int J. Multi-Phase Flow*, **24**, 1005 (1998).

Buscall, R., and L. R. White, "The Consolidation of Concentrated Suspensions," *J. Chem. Soc. Faraday Transactions,* **83**, 873 (1987).

DeKretser, R., S. P. Usher, P. J., Scales, K. A., Landman, and D. V. Boger, "Rapid Filtration Measurement of Dewatering Design and Optimisation Parameters," *AIChE J.*, **47**(8), 1758 (2001).

Howells, I., A. Landman, K. A. Panjkov, C. Sirakoff., and L. R. White "Time-Dependent Batch Settling of Flocculated Suspensions," *Appl. Math. Modelling,* **14**,77 (1990).

Landman, K. A., and W. B. Russel, "Filtration at Large Pressures for Strongly Flocculated Suspensions," *Phys. Fluids A*., **5** (3) 550 (1993).

Landman, K. A., C. Sirakoff, and L. R White, "Dewatering of Flocculated Suspensions by Pressure Filtration," *Phys. Fluids A*, **3** (6), 1495 (1991).

Landman, K. A. and L. R.White, "Predicting Filtration Time and Maximising Throughput in a Pressure Filter," *AIChE J.,* **43**(12), 3147 (1997).

Landman, K. A., L. R. White, and R. Buscall, "The Continuous Flow Gravity Thickener, Steady State Behaviour," *AIChE J.,* **34**(2), 239 (1988).

Press, W. H., S. A. Teukolsky, W. T. Vetterling, and B. P. Flannery, *Numerical Recipes in Fortran 77 2nd Edn.*, Cambridge University Press (1996).

Richardson, J. F., and W. N. Zaki, "Sedimentation and Fluidisation: Part 1," *Trans. Inst. Chem. Engs.,* **32**, 35 (1954).

Wakeman, R. J., and E. S. Tarleton, "Modelling, Simulation and Process Design of the Filter Cycle," *Industrie Minerale-Mines et Carrières: Les Techniques*, 5, July (1991).

Manuscript received Jan. 12, 2003, and revision received Sept. 10, 2003.